Desalination 333 (2014) 36–44

Contents lists available at ScienceDirect

Desalination

journal homepage: www.elsevier.com/locate/desal

Studies on fouling by natural organic matter (NOM) on polysulfone membranes: Effect of polyethylene glycol (PEG)

Muhamad Zaini Yunos [a,b], Zawati Harun [a,b,*], Hatijah Basri [c], Ahmad Fauzi Ismail [d]

[a] ENIGMA, Department of Materials and Design, Faculty of Mechanical and Manufacturing, Universiti Tun Hussein Onn Malaysia, Parit Raja, Batu Pahat 86400, Johor, Malaysia
[b] Integrated Material Process, Advanced Materials and Manufacturing Center, Universiti Tun Hussein Onn Malaysia, Parit Raja, Batu Pahat 86400, Johor, Malaysia
[c] Department of Technology and Heritage, Faculty of Science, Technology and Human Development, Universiti Tun Hussein Onn Malaysia, Parit Raja, Batu Pahat 86400, Johor, Malaysia
[d] Advanced Membrane Technology Research Centre, Faculty of Chemical and Natural Resources Engineering, Universiti Teknologi Malaysia, Skudai, 81300 Johor Bahru, Johor, Malaysia

HIGHLIGHTS

- Fouling behaviour of PSf by NOM
- Different concentrations and molecular weights of PEG were used as additives in membrane.
- Detailed morphology and membrane performance were characterized and measured.
- Real river water which possesses hydrophobic and hydrophilic characteristics was used to evaluate membrane fouling.

ARTICLE INFO

Article history:
Received 19 July 2013
Received in revised form 21 October 2013
Accepted 10 November 2013
Available online 14 December 2013

Keywords:
PSf membrane
PEG
NOM
Fouling

ABSTRACT

Polysulfone membranes were prepared via phase inversion technique by using polyethylene glycol with molecular weights of 400, 1500 and 6000 Da as pore forming agent in dope formulation. The performance of membrane was characterized using humic acid and water sample taken from Sembrong River, Johor, Malaysia was used as natural organic matter sources. Membrane properties were also characterized in terms of mean pore radius, pure water flux, humic acid rejection and fouling resistance. The results indicated that the pure water flux and mean pore radius of membranes increased with the increase of PEG content. Fourier transform infrared spectroscopy results revealed the presence of hydrophilic component in PSf/PEG blend with the significant appearance of O–H peak at 3418.78 cm^{-1}. Scanning electron microscopy analysis revealed the presence of finger-like structure for all membranes and the structure intensified as PEG content was increased. The results obtained from the fouling study indicated that the membrane with the lowest PEG content and molecular weight has an excellent performance in mitigating fouling.

1. Introduction

Natural organic matter (NOM) is one of the major pollutants in acidic and low turbidity water source. In Malaysia, most of the water sources are contaminated with NOM especially that from peat soil. Natural organic compounds such as humic acid and fulvic acid contributed to the natural colour of water (brown to black) which becomes more visible if the dissolved organic carbon (DOC) exceeds 5 mg/L. Therefore, the removal of NOM is usually known as colour removal. According to Thurman [1], surface water in average contains about 45% fulvic acid, 5% humic acid, 25% low molecular weight acid, and the remaining consists of neutral compounds, bases and contaminants. Although these compounds are relatively harmless, they are able to form carcinogenic disinfection byproducts such as trihalomethanes [2,3]. In order to remove these substances and render environmental remediation, ultrafiltration (UF) has been recognised as one of the attractive approaches that has been highlighted in many studies due to its compactness, easy automation, high removal rate of organic matter and also capability to remove virus [4].

Polysulfone (PSf) is the most commonly used polymer in the fabrication of UF membrane. PSf is known for its resistance in extreme pH condition and high thermal stability [5]. However, one of the major problems of polysulfone is its hydrophobic characteristic which often causes hydrophobic particle to adsorb on the surface of the PSf membrane. This phenomenon had led to membrane fouling and drastically decreased the membrane permeability.

Fouling is described as pore-blocking, solute aggregation or adsorption phenomenon. Irreversible membrane fouling by proteins, NOM and other biomolecules' adsorption reduces the flux of membrane and

* Corresponding author at: Integrated Material Process, Advanced Materials and Manufacturing Center, Universiti Tun Hussein Onn Malaysia, Parit Raja, Batu Pahat 86400, Johor, Malaysia. Tel.: +60 74537608; fax: +60 74536080.
E-mail addresses: mzaini@uthm.edu.my (M.Z. Yunos), zawati@uthm.edu.my (Z. Harun), hatijah@uthm.edu.my (H. Basri), afauzi@utm.my (A.F. Ismail).

0011-9164/$ – see front matter © 2013 Elsevier B.V. All rights reserved.
http://dx.doi.org/10.1016/j.desal.2013.11.019

hinders the wide scale application of UF membranes [6,7]. The current technique to counter this problem is by cleaning the membrane with aggressive chemicals such as hypochlorite, nitric acid, sodium hydroxide and oxalic acid at extreme pH [8,9]. These chemicals can only remove the adsorbed foulants for some time and the membrane must be replaced when this cleaning method becomes ineffective. The mechanisms and causes of fouling that strongly depend on the membrane surface characteristic (hydrophilicity, charge and roughness), concentration polarization, cake layer formation, foulant properties and water chemistry have been well studied and reported [7,10–12]. Among all these causes, membrane surface seems to be the most crucial factor to be looked into since the properties of membrane surface could potentially affect the overall performance of the resultant membranes. Surface modifications of membrane to obtain high hydrophilicity, low surface roughness and positive charge have been progressively investigated in order to produce a membrane with high antifouling properties [13–15].

A membrane with good rejection and water permeability is usually prepared by incorporating suitable additive through an efficient fabrication method. Various types of additive such as mineral fillers, polymer, salts, non-solvent and solvent were incorporated using different approaches to improve the membrane properties [16–19]. Generally, inorganic and mineral fillers are used to enhance and create stability to the membrane performances. Hamid et al. reported that the addition of titanium dioxide nanoparticle in polysulfone has reduced the fouling resistance of the membrane [20]. They also found that the additive has increased rejection of humic acid up to 90%. Idris et al. studied the effect of lithium bromide salts on the performance of a polyethersulfone hollow fibre membrane and found that lithium bromide enhanced membrane hydrophilicity and water permeability [21]. The capability of a strong non-solvent such as water as an additive in the membrane performance was studied by Yunos et al. [22]. They discovered that by adding water in PSf dope formulation, pure water flux was greatly enhanced despite the deterioration in the strength of the membrane. Typically, a low molecular weight polymer is used as an additive to improve the pore forming of the membrane. Polyvinyl pyrrolidone (PVP) and polyethylene glycol (PEG) are the most common additives used in membrane formulation [23–26]. Investigation of PEG as an additive has attracted enormous attentions from many researchers due to the ease of preparation as PEG can dissolve in water and organic solvent, low toxicity and cost [26–29]. PEG has shown promising potential in increased membrane pore size and permeability. Ma et al. have studied the effect of PEG on the resultant PSf membrane and they found that the presence of PEG has greatly improved the membrane hydrophilicity, porosity and water permeability [27]. The addition of PEG has also reduced the thermodynamic stability of dope formulation which then led to finger-like formation in the membrane structure [26].

According to some previous reports [16,30,31], surface-bound long-chain hydrophilic molecules in PEG were sufficient to form steric repulsion which prevents adsorption of protein molecules onto membrane. Zhu et al. [32] found that the addition of PEG in membrane could reduce the total adsorption of bovine serum albumin (BSA) on the membrane surface. Kim et al. [33] prepared a surface-coated membrane using PEG hydrogel on reverse osmosis (RO) membrane and demonstrated fouling reduction of salt water as foulant. Grafting of PEG on membrane surface was also found effective to reduce at least 96% BSA adhesion as studied by McCloskey et al. [34]. They found that grafted PEG created hydration shell that renders surface resistant to BSA adsorption.

As far as we are concerned, the investigations in the effect of PEG concentration on the performance of membrane for NOM removal and fouling mitigation were rarely studied. Thus, in this work, the fouling behaviour of the PSf membrane with PEG as an additive was studied by using NOM source from real river water. The prepared membranes were characterized via scanning electron microscopy (SEM) and Fourier transform-infrared spectroscopy (FTIR) to provide further insights in the fouling mechanism of PSf membrane.

Table 1
Composition of casting solution.

	PSf	NMP	PEG 400[a]	PEG 1500[a]	PEG 6000[a]
P.4.400	18	82	4	-	-
P.8.400		82	8	-	-
P.10.400		82	10	-	-
P.12.400		82	12	-	-
P.16.400		82	16	-	-
P.10.1500		82	-	10	-
P.10.6000		82	-	-	10

[a] Represent molecular weight (Da).

2. Experimental

2.1. Materials

Polymer solutions were prepared using polysulfone (UDEL P1700) as polymeric material and N-methyl-2-pyrrolidone (NMP) (MERCK) as solvent. Meanwhile PEG 400, 1500 and 6000 (Qrec) were used as an additive. Distilled water was used as a non-solvent bath for the purposes of phase inversion. All chemicals purchased in this study were used without any further purification.

2.2. Membrane preparation

In this study, PSf/PEG flat sheet membranes were prepared by casting a polymer solution (18 wt.% of PSf) with different PEG contents and molecular weights on a glass plate. Table 1 shows the composition of various polymer solutions prepared in this study. Polymer solution was cast on the glass plate with casting knife gap setting at 150 μm with an appropriate casting shear. The cast solution was then immersed in water bath until the membrane thin film peels off naturally. The procedures were conducted at constant temperature and relative humidity (HR) (25 °C; HR 84%).

2.3. Scanning electron microscopy (SEM)

SEM JEOL GSM was used to examine the morphology of membrane. The membrane was immersed in liquid nitrogen and fractured

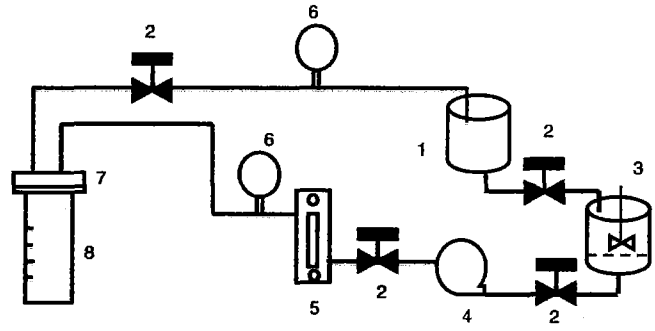

Fig. 1. Ultrafiltration permeation testing unit schematic diagram, (1) feed tank; (2) control valve;(3) pre-treatment tank; (4) osmotic pump; (5) flow meter; (6) pressure gauge; (7) filter holder; (8) beaker for collecting permeate.

Table 2
Surface water characteristic after prefiltration process.

UV_{254} (cm^{-1})	0.178 ± 0.006
DOC (mg/L)	9.87 ± 1.42
Turbidity (NTU)	16 ± 4.2
Mn^{2+} (mg/L)	0.442
Fe^{2+} (mg/L)	3.273
Al^{3+} (mg/L)	6.435
Hydrophilic DOC %	32.5%
Hydrophobic DOC %	42.3%

carefully. The fractured samples were then gold sputtered prior to the scanning.

2.4. Fourier transform infrared (FTIR)

FTIR (Perkin Elmer Spectrum 100) was employed to detect and analyse the functional groups within the molecules of the polymer based structure in the prepared membrane. The membranes were characterized using the attenuated total reflectance (ATR) technique at a 4.0 cm^{-1} resolution and the results of 32 scans were recorded.

2.5. Membrane mean pore radius (r_m)

In order to determine the membrane mean pore radius, the porosity of the membrane was first being determined. The membrane was first immersed in distilled water for 24 h at 25 °C. The membrane surface was then wiped carefully with tissue paper prior to the weighing with electronic balance, and the initial weight was denoted as W_w. This wet membrane was dried in an oven at 60 °C for 24 h and it was weighed again in dry state, denoted as W_d. Membrane porosity was determined by using the following equation:

$$\varepsilon = \frac{(W_w - W_d)}{(\rho_w \times V)} \quad (1)$$

where W_w is the weight of wet membranes (g), W_d is the weight of dry membranes (g), ρ_w is the density of pure water at room temperature (g/cm^3) and V is the volume of membrane in wet state (cm^3). In order to minimize the experimental errors, each measurement was repeated for five times and the average was calculated.

Mean pore radius was determined by using the filtration velocity method as stated in the Guerout–Elford–Ferry equation [24]:

Mean pore radius, r_m:

$$r_m = \sqrt{\frac{(2.9 - 1.75\varepsilon) \times 8\eta l Q}{\varepsilon \times A \times \Delta P}} \quad (2)$$

where η is the water viscosity, l is the membrane thickness, Q is the volume of permeate water per-unit time, A is the membrane area and ΔP is the operational membrane pressure.

2.6. Permeation flux, rejection and fouling investigation

The permeation flux and rejection of membrane were measured based on the ultrafiltration experimental set-up. The schematic of the experimental set up is presented in Fig. 1. The determination of

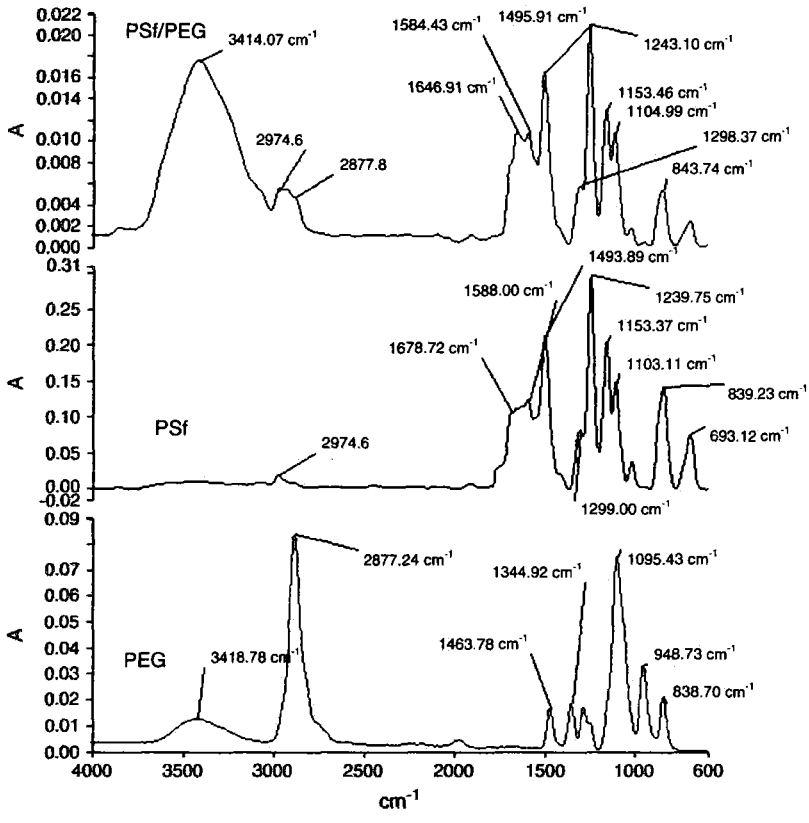

Fig. 2. FTIR results.

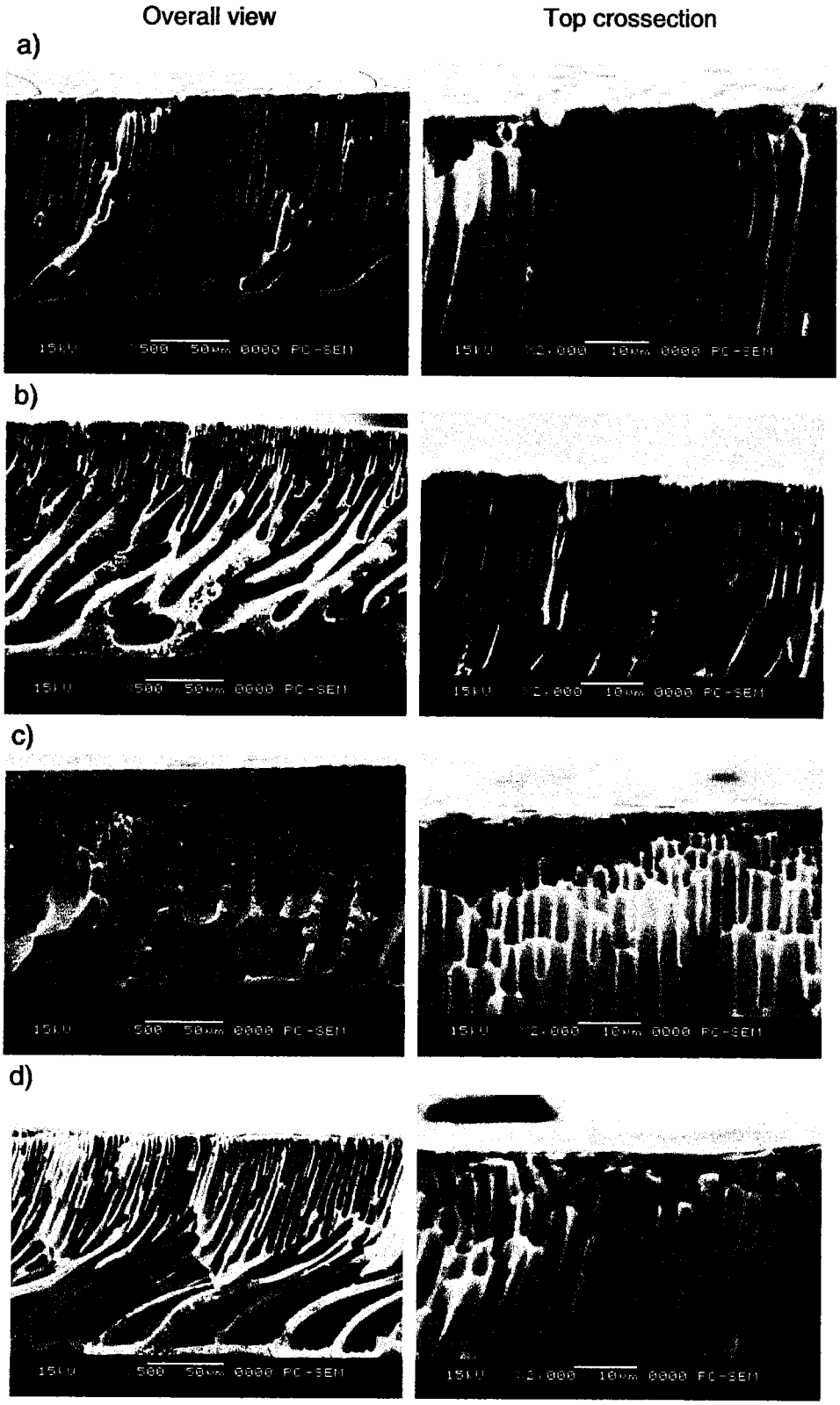

Fig. 3. Scanning electron micrograph image at top and overall membrane cross section of PSf/PEG at different PEG contents; a) 4 wt.%, b)8 wt.%, c)10 wt.%, d)16 wt.%.

pure water flux by using distilled water as feed was conducted at pressure 200 kPa. The flux was calculated using Eq. (3):

$$PWF = \frac{Q}{(A \times \Delta t)} \quad (3)$$

where PWF is the pure water flux (L/m^2h), Q is the permeate volume (L), A is the membrane area (m^2), and Δt is the permeate time (h).

Rejection was characterized using 100 mg/L humic acid and Sembrong river water, Johor, Malaysia was used as feed solution. Membrane was first filtered with distilled water until the flux is steady. The

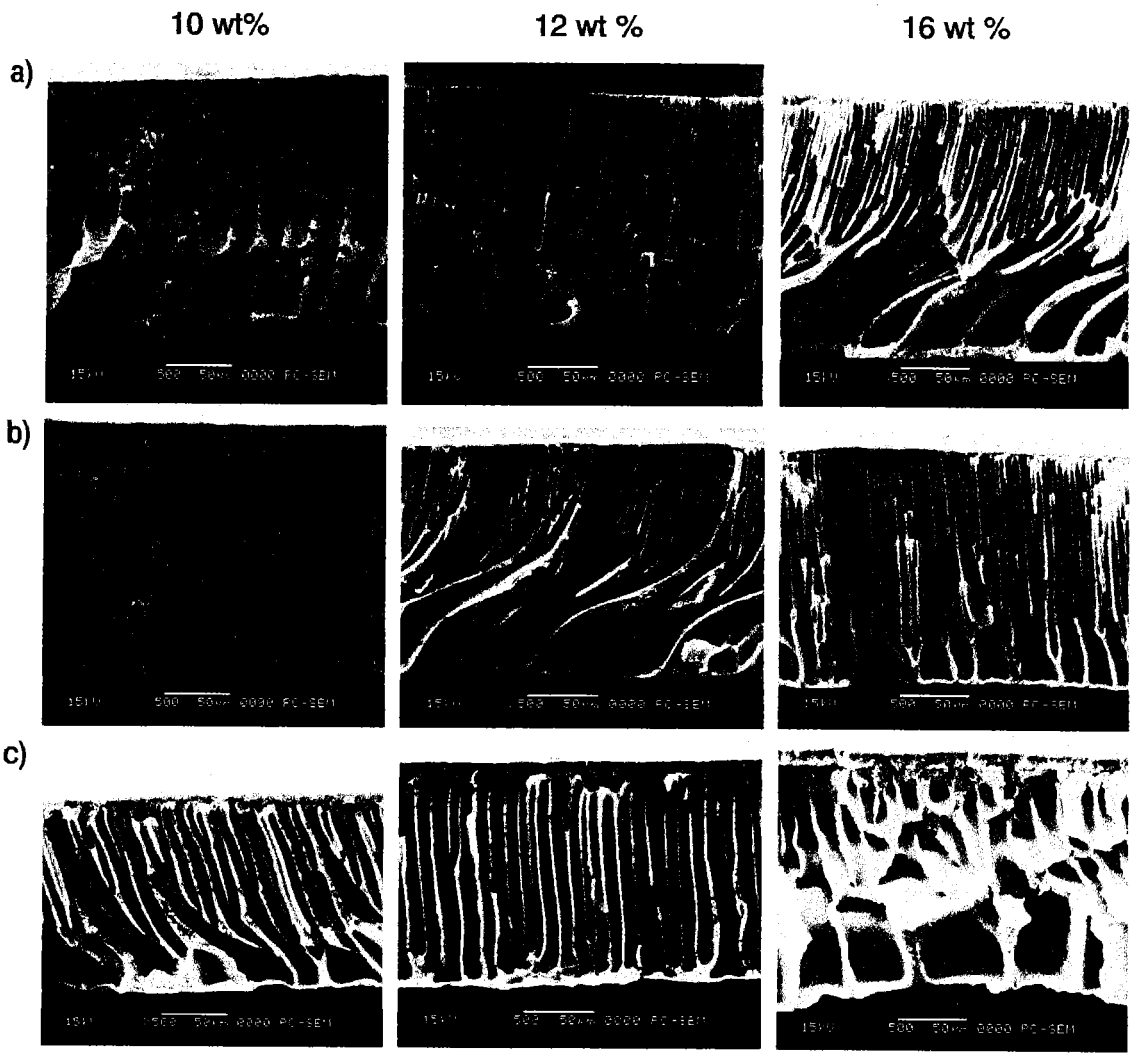

Fig. 4. SEM image of PSf/PEG at different PEG contents and molecule weights: a)400 Da, b)1500 Da, c)6000 Da.

concentrations of feed and permeate solutions were determined by using a UV spectrophotometer (Thermo Scientific, Genesys 10S) and total organic carbon (Shimadzu, TOC-VCSH) which was calculated using Eq. (4):

$$\%R = \left(1-\frac{C_p}{C_f}\right) \times 100 \quad (4)$$

where %R is the rejection percentage, C_p is the permeate concentration and C_f is the feed concentration.

The capability of the prepared membrane to resist NOM water source was investigated. Fouling can be measured by membrane resistance during ultrafiltration process. This resistance is due to the cake layer formation on membrane surface and impurities adsorption onto or within membrane pores. Therefore to determine

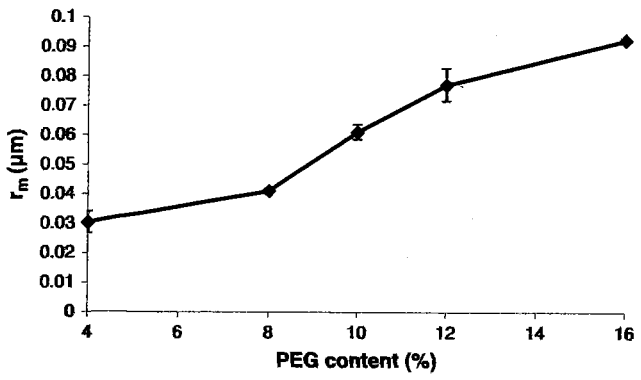

Fig. 5. Mean pore radius of PSf/PEG 400 membrane at different PEG concentrations.

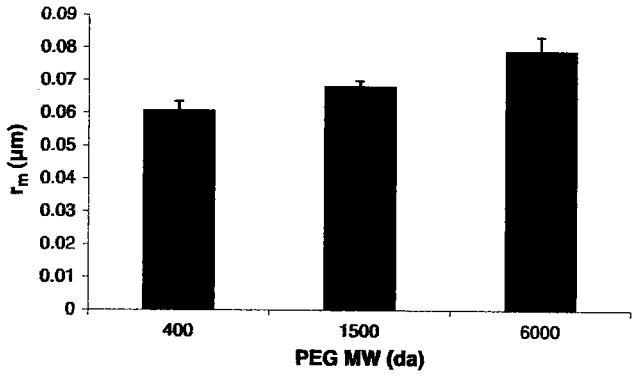

Fig. 6. Mean pore radius of PSf/PEG membrane for 10 wt.% PEG content at different PEG molecular weights.

fouling resistance of membrane, Darcy's Law was used as shown in Eq. (5) [20]:

$$J = \frac{\Delta P}{\mu R_t} = \frac{\Delta P}{\mu\left(R_m + R_{cp} + R_c + R_a\right)} \quad (5)$$

where J is flux, μ is the viscosity of permeate, ΔP is the transmembrane pressure, and R_t is the total filtration resistance of the membrane. Meanwhile R_m, R_{cp}, R_c and R_a are intrinsic membrane resistance, membrane resistance due to concentration polarization, cake layer formation and adsorption, in particular order.

The membrane was first subjected to a pressure of 200 kPa and the feed temperature at 20 °C. The distilled water was then replaced with the river water sample at the same operating pressure. The stable water flux using distilled water was recognised as J_{PWF}. The permeate readings were then periodically taken for every 5 min interval time throughout 120 min of filtration duration. After 120 min of filtration, the permeate flux was recorded and known as J_{cp}. The membrane was rinsed with distilled water to remove concentration polarization layer for 10 min and pure water flux was measured again and labelled as J_c. Lastly, the membrane was washed with a 0.1 M HCl solution for 10 min and the PWF was measured and recorded as J_a. HCl was used in this study as a chemical cleaning agent in order to remove any foulant adsorption on membrane surface. Individual resistant membrane was then calculated using the following equations:

$$R_m = \frac{\Delta P}{\mu J_{PWF}} \quad (6)$$

$$R_{cp} = \frac{\Delta P}{\mu J_a} - R_m \quad (7)$$

$$R_c = \frac{\Delta P}{\mu J_c} - R_m - R_{cp} \quad (8)$$

$$R_a = \frac{\Delta P}{\mu J_{cp}} - R_m - R_{cp} - R_c. \quad (9)$$

2.7. Sembrong surface water quality

The surface water used in this study was taken from Sembrong River at Parit Raja, Johor, Malaysia. The river source water was found to be soft and rich in NOM. The characteristics of the surface water are summarised in Table 2. The raw water was pre-filtered with 0.5 μm ceramic microfiltration to remove the particulate materials. The UV_{254nm} absorbance was measured using a Thermo Scientific, Genesys 10S UV–Vis spectrophotometer at a wavelength of 254 nm. Concentration of heavy metal was determined using Hach DR5000. The hydrophilicity/hydrophobicity of NOM fraction characteristic was based on DOC and mass balance technique with DAX-8 and XAD-4 resins [35].

3. Results and discussions

3.1. Fourier transform-infrared spectroscopy (FTIR)

The FTIR spectra for the prepared membranes are depicted in Fig. 2. The aromatic vibration ether band of PSf is detected at around 1241 cm^{-1}. The SO_2 groups' stretching vibration is around 1300 cm^{-1}. The absorptions at 1900 cm^{-1}, 1775 cm^{-1}, 1605 cm^{-1}, 1488 cm^{-1} and 1169 cm^{-1} are resulted from the aromatic ring of PSf. The vibration at 2968 cm^{-1} is attributed to the two methyl groups of PSf. PEG with a chemical structure of (HO–CH_2–(CH_2–O–CH_2)n–CH_2–OH) has resulted in significant peaks. The peaks at 1050 cm^{-1} to 1150 cm^{-1} were due to the stretching of ether groups, with a maximum peak at

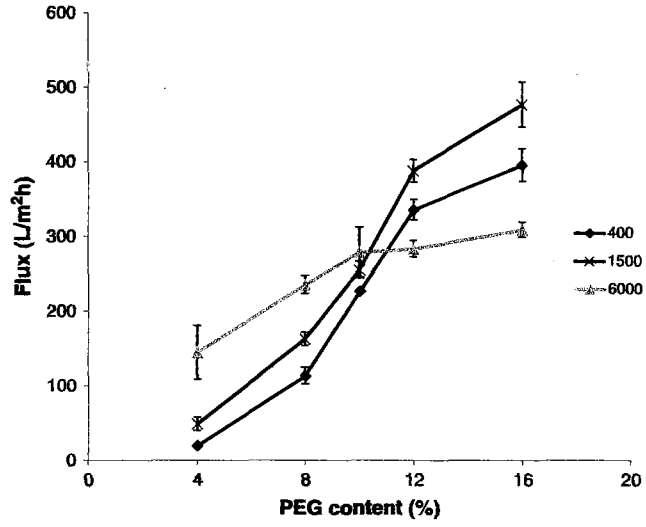

Fig. 7. Pure water flux of PSf at different PEG contents and molecular weights.

$\nu = 1150$ cm^{-1}. Alkyl (R–CH_2) stretching vibration is observed at around 2850–3000 cm^{-1}. The spectrum also shows a broad absorption band for hydroxyl group at $\nu = 3200$–3600 cm^{-1}. Advantageously, PEG possesses both hydrophilic and hydrophobic properties thus giving them a unique ability to dissolve in both aqueous and organic solvents. Thus it could be homogenously mixed with PSf in NMP solution. The peak around 2877.20 cm^{-1} is assigned to N–CH_3 (aliphatic) stretching vibration and this signifies the presence of PEG in PSf blend. The presence of OH vibration peak at 3418.78 cm^{-1} for PSf/PEG membranes also indicates that they are able to interact with water and perform as a hydrophilic membrane. The findings are in accordance with those reported elsewhere [17,36] and it is believed that this characteristic has contributed to an increase of pure water flux of the PSf/PEG membrane, which will be further discussed in the following section.

3.2. Morphological properties of membranes

Fig. 3 represents the SEM micrographs of the cross section of the PSf membrane at different PEG concentrations. Observation on the membrane structure showed that all prepared membranes have asymmetric porous substructure with a dense skin layer. This membrane structure is

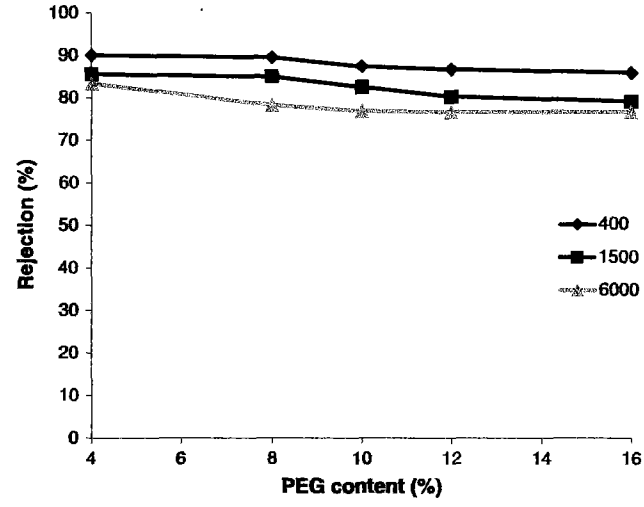

Fig. 8. Humic acid rejection of PSf membrane at different PEG contents and molecular weights.

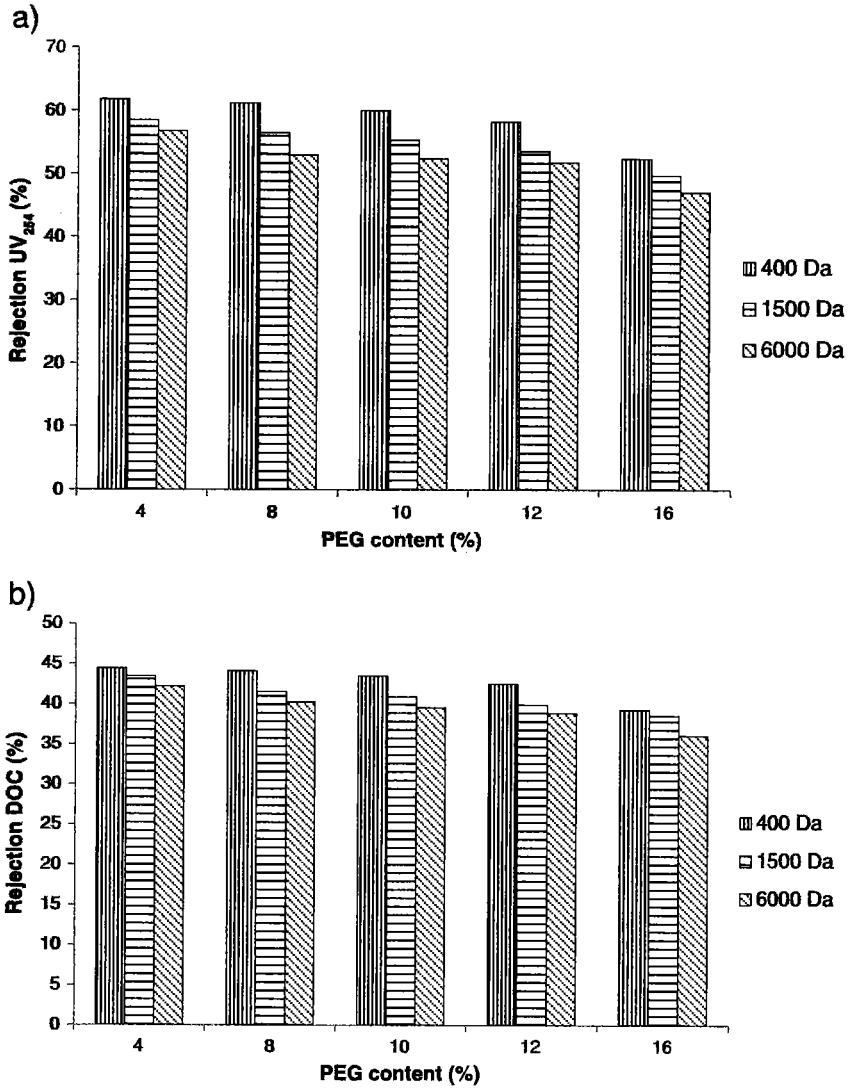

Fig. 9. UV_{254} (a) and DOC (b) Sembrong water rejection of PSf membrane at different PEG contents and molecular weights.

generally governed by the interaction between the polymer solution, non-solvent and kinetic process during phase inversion process [37]. The addition of PEG in PSf membrane increased the finger-like structure at the top of the membrane. This could be due to dope solutions that become thermodynamically less stable with the presence of PEG [27,29].

Fig. 4 shows the cross section images of the PSf membrane at different PEG molecular weights and contents. The figures show similar trend for PEG 400 and PEG 1500, however as PEG 6000 content increased from 10 wt.% to 16 wt.%, the dense layer of PSf becomes thicker and the sponge-like structure can be more clearly seen. Formation of membrane depends on the solubility and diffusivity between polymer, solvent and non-solvent [38]. When membrane dope was cast and immersed in water bath, the low molecular weight PEG and NMP diffused in water instantaneously from dope solution and PSf solidified to form a finger-like structure. However, as PEG molecular weight increased, the PEG diffusion to water becomes slower due to the low solubility between PEG and water, hence resulted in thick sponge-like structure formation in the top layer of the membrane. A similar observation has been reported by Li et al. [39] using PEG as additive and dimethyl acetamide (DMac) as solvent.

Fig. 4 shows that the size of the finger-like structure at the intermediate layer becomes larger with the increasing PEG molecular weight. The membrane solidification usually starts at the membrane's outer surface due to thermodynamic instability between dope solution and water. Then it is followed by diffusion of solvent into water and water into membrane film. As water starts to penetrate into the membrane, droplets are formed and bind together to solidify at the inner surface of the membrane. In the meantime, solvent tends to diffuse towards outer membrane. This mechanism leads to the formation of solidified walls of finger-like structure [19]. The size of the finger-like structure depends on the diffusion rate of discharge solvent towards the outer surface of the membrane. Due to the low solubility of PEG in water at high PEG molecular weight, diffusion between solvent and non-solvent became slower and the wall created between PSf and water became larger. In such situation, a larger finger-like structure is formed.

3.3. Mean pore radius, water permeability and rejection test

The performance of the prepared membranes was characterized in terms of mean pore radius, water permeability and rejection test. Fig. 5 shows the mean pore radius of the PSf/PEG membrane at different PEG contents. As demonstrated from the figure, membrane mean pore radius increased as the PEG content increased. This is due to the

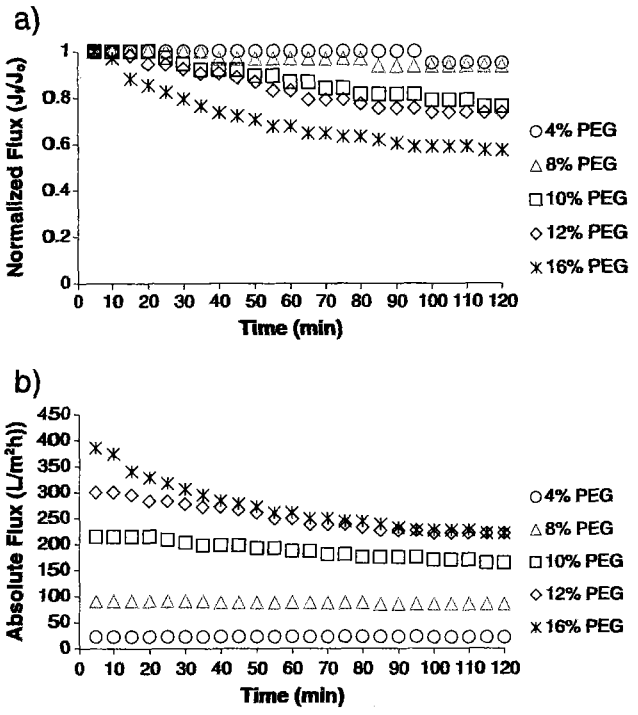

Fig. 10. Performance of PSf/PEG 400 ultrafiltration membrane at different PEG contents: a) Normalized flux, b) Absolute flux.

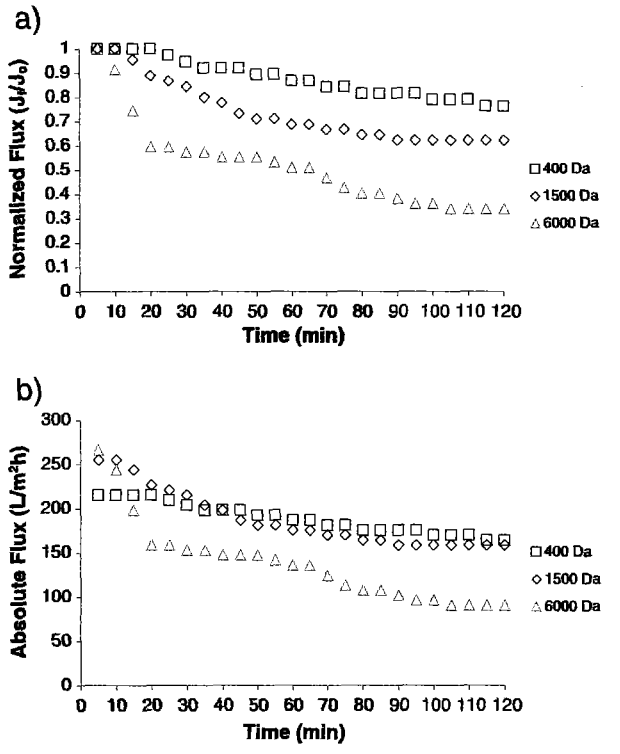

Fig. 11. Performance of PSf/10 wt.% PEG ultrafiltration membrane at different PEG molecular weights: a) Normalized flux, b) Absolute flux.

formation of a finger-like and macrovoid structure that enhanced the membrane mean pore radius. The same trend is also observed at different PEG molecular weights with fixed PEG content (10 wt.%) as shown in Fig. 6.

PWF of all membranes added with different PEG contents and molecular weights is presented in Fig. 7. These results demonstrated that, water permeability increased as PEG content increased regardless of the PEG molecular weight and content. However for PEG 6000, the PWF start to level off at 10% PEG content. The figure also shows that with addition of PEG at 12 wt.% and 16 wt.%, the membrane incorporated with PEG 6000 shows lower flux as compared to PEG 1500 and PEG 400. In general, The increment of water permeability in the membrane is due to the increased membrane pore size and improved surface hydrophilicity. This unexpected trend for PEG 6000 might be due to the formation of a thick sponge-like structure at the top layer of membrane as observed in SEM images. This is in line with the findings reported by Hua et al. who found that high molecular weight of PEG may contribute to the deterioration of the membrane pure water flux [36].

Humic acid rejection exhibited by PSf membrane with different PEG contents and molecular weights is shown in Fig. 8. As shown in the figure, the humic acid rejection by PSf membrane was slightly decreased as the PEG 400 content increased. This is due to the undesired trade-off effects, in which the rejection decreases as the flux increases. The mean pore radius increment has also contributed to the decrease of humic acid rejection as larger pore size allowed more humic acid molecule to pass through the membrane. The same phenomenon was observed for addition of PEG 1500 and PEG 6000 in membrane. The result shows that addition of PEG 400 in membrane has excellent humic acid rejection as compared to PEG 1500 and PEG 6000. A similar trend was found by Ma et al. who used BSA and pepsin as rejection model [27].

NOM rejection of the membranes is illustrated in Fig. 9. Fig. 9(a) represents UV_{254} rejection and Fig. 9(b) shows DOC rejection The highest rejection of NOM is shown at 61.8% (UV_{254}) and 44.4% (DOC) for PSf with 4% PEG 400 content. The overall results show that UV_{254} rejection has higher rejection as compared to DOC. This suggests that the prepared membrane was able to remove aromatic compound such as hydrophobic acid which contributes 42.3% DOC in river water (Table 2). The figure also indicates that NOM rejection decreased as PEG content and molecular weight increased. As compared to humic acid rejection, the rejection performance was significantly affected by the increasing PEG content and molecular weight. This is due to the fact that NOM contains several compounds such as humic acid, tannic acid, protein and carbohydrate with various sizes and charges. These various sizes and electrostatic charges of solute molecule might affect the performance of the membrane, in terms of declination of membrane rejection. On the other hand, small sizes of the NOM molecule will pass through the membrane and the hydrophobic NOM molecules showed high tendency to be adsorbed inside the membrane [40,41].

Table 3
Individual filtration resistant of membrane.

	R_m (10^{12} m^{-1})	R_{sp} (10^{12} m^{-1})	R_c (10^{12} m^{-1})	R_s (10^{12} m^{-1})
P.4.400	21.388 (±0.221)	9.166 (±0.268)	0.258 (±0.184)	0.263 (±0.102)
P.8.400	7.575 (±0.171)	0.161 (±0.141)	0.168 (±0.104)	0.175 (±0.091)
P.10.400	3.189 (±0.113)	0.1151 (±0.157)	0.0926 (±0.088)	0.781 (±0.101)
P.12.400	2.818 (±0.322)	0.0671 (±0.282)	0.144 (±0.087)	1.149 (±0.112)
P.16.400	1.954 (±0.125)	0.0212 (±0.321)	0.0439 (±0.077)	1.652 (±0.373)
P.10.1500	2.693 (±0.175)	0.336 (±0.164)	0.131 (±0.087)	1.166 (±0.258)
P.10.6000	2.286 (±0.183)	0.743 (±0.129)	0.159 (±0.097)	4.385 (±0.348)

3.4. Fouling investigation

Fig. 10 presents the normalized and absolute flux for the PSf membrane with different PEG 400 contents. As shown in the figure, the flux of the membrane reduced with time. It is noticed that the flux significantly reduced as the PEG content increases in the membrane. Even though the membrane incorporated with 4 wt.% PEG has the lowest flux, the flux is more stable as compared to the membrane incorporated with 16 wt.% PEG. These results indicate that the addition of PEG increased the membrane fouling. The observed results are in contradiction with the previous results reported by Kim et al. in which PEG could

enhance membrane antifouling [33]. This might be due to variation of the type of foulant used in different studies. Table 3 gives the value of individual filtration resistance of the membrane with different PEG contents. It was noticed that PEG addition reduced intrinsic membrane resistance but increased adsorption resistance of the membrane. The figure also shows that contribution of fouling resistance due to concentration polarization and cake layer formation is not significant as compared to resistance due to fouling caused by membrane adsorption. This phenomenon is due to the existence of hydrophilic and hydrophobic substances in the river water sample. These substances tend to adsorb easily on the membrane surface and subsequently foul the membrane. As the pore size increased in the membrane, tendency for adsorption of this substance also increased. This aspect is clearly observed for fouling behaviour at different PEG molecular weights as shown in Fig. 11 and Table 3. Normalized flux for PEG 6000 is drastically reduced to 63% for 20 min due to the membrane fouling. Meanwhile PEG 400 shows excellence normalized flux as compared to PEG 1500 and PEG 6000. As shown in Table 3, even though PEG 6000 shows the lowest intrinsic membrane resistance, it has the highest resistance towards the fouling that was due to adsorption, cake formation and concentration polarization.

4. Conclusions

The effects of different PEG contents and molecular weights to the PSf membrane in respect to morphology, flux, rejection and fouling were investigated. It was found that PEG enhanced pore formation of the membrane. As PEG molecular weight increased, a finger-like and dense layer structure also enhanced. The same effect was also noticed for the membrane water flux. In the case of PEG 6000, the flux started to level off at 10 wt.% PEG content. Overall rejection of membrane decreased as PEG content and molecular weight increased for both humic acid and Sembrong River water sample. PEG enhanced pore formation of the membrane but increased the fouling properties of the membrane.

Acknowledgement

The authors thank the financial support for the LRGS Vot A022 grant and the FRGS Vot 0754 grant that were sponsored by the Ministry of Higher Education Malaysia (MOHE).

References

[1] E.M. Thurman, Preparative isolation of aquatic humic substance, Environ. Sci. Technol. 15 (1981) 468–466.
[2] A. Matilainen, E.T. Gjessing, T. Lahtinen, L. Hed, A. Bhatnagar, M. Sillanpää, An overview of the methods used in the characterisation of natural organic matter (NOM) in relation to drinking water treatment, Chemosphere 83 (2011) 1431–1442.
[3] H. Wong, K.M. Mok, X.J. Fan, Natural organic matter and formation of trihalomethanes in two water treatment processes, Desalination 210 (2007) 44–51.
[4] M. Mulder, Basic Principles of Membrane Technology, 2nd ed. Kluwer Academic, London, 1996.
[5] S.P. Nunes, K.V. Peinemann, Membrane Technology in the Chemical Industry, 2006.
[6] S. Lee, C.-H. Lee, Effect of membrane properties and pretreatment on flux and NOM rejection in surface water nanofiltration, Sep. Purif. Technol. 56 (2007) 1–8.
[7] X. Wei, R. Wang, Z. Li, A.G. Fane, Development of a novel electrophoresis–UV grafting technique to modify PES UF membranes used for NOM removal, J. Membr. Sci. 273 (2006) 47–57.
[8] S.K.S. Al-Obeidani, H. Al-Hinai, M.F.A. Goosen, S. Sablani, Y. Taniguchi, H. Okamura, Chemical cleaning of oil contaminated polyethylene hollow fiber microfiltration membranes, J. Membr. Sci. 307 (2008) 299–308.
[9] W.S. Ang, N.Y. Yip, A. Tiraferri, M. Elimelech, Chemical cleaning of RO membranes fouled by wastewater effluent: achieving higher efficiency with dual-step cleaning, J. Membr. Sci. 382 (2011) 100–106.
[10] A.W. Zularisam, A.F. Ismail, M.R. Salim, M. Sakinah, T. Matsuura, Application of coagulation–ultrafiltration hybrid process for drinking water treatment: optimization of operating conditions using experimental design, Sep. Purif. Technol. 65 (2009) 193–210.
[11] W. Shi, M.M. Benjamin, Membrane interactions with NOM and an adsorbent in a vibratory shear enhanced filtration process (VSEP) system, J. Membr. Sci. 312 (2008) 23–33.
[12] J.-y. Tian, Y.-p. Xu, Z.-l. Chen, J. Nan, G.-b. Li, Air bubbling for alleviating membrane fouling of immersed hollow-fiber membrane for ultrafiltration of river water, Desalination 260 (2010) 225–230.
[13] L.-J. Mu, W.-Z. Zhao, Hydrophilic modification of polyethersulfone porous membranes via a thermal-induced surface crosslinking approach, Appl. Surf. Sci. 255 (2009) 7273–7278.
[14] A.V.R. Reddy, D.J. Mohan, A. Bhattacharya, V.J. Shah, P.K. Ghosh, Surface modification of ultrafiltration membranes by preadsorption of a negatively charged polymer: I. Permeation of water soluble polymers and inorganic salt solutions and fouling resistance properties, J. Membr. Sci. 214 (2003) 211–221.
[15] D. Rana, T. Matsuura, Surface modifications for antifouling membranes, Chem. Rev. 110 (2010) 2448–2471.
[16] Z. Peng, L.X. Kong, A thermal degradation mechanism of polyvinyl alcohol/silica nanocomposites, Polym. Degrad. Stab. 92 (2007) 1061–1071.
[17] E. Yuliwati, A.F. Ismail, Effect of additives concentration on the surface properties and performance of PVDF ultrafiltration membranes for refinery produced wastewater treatment, Desalination 273 (2011) 226–234.
[18] M.A. Aroon, A.F. Ismail, M.M. Montazer-Rahmati, T. Matsuura, Morphology and permeation properties of polysulfone membranes for gas separation: effects of non-solvent additives and co-solvent, Sep. Purif. Technol. 72 (2010) 194–202.
[19] A. Mansourizadeh, A.F. Ismail, Preparation and characterization of porous PVDF hollow fiber membranes for CO2 absorption: effect of different non-solvent additives in the polymer dope, Int. J. Greenhouse Gas Control 5 (2011) 640–648.
[20] N.A.A. Hamid, A.F. Ismail, T. Matsuura, A.W. Zularisam, W.J. Lau, E. Yuliwati, M.S. Abdullah, Morphological and separation performance study of polysulfone/titanium dioxide (PSF/TiO2) ultrafiltration membranes for humic acid removal, Desalination 273 (2011) 85–92.
[21] A. Idris, I. Ahmed, M. Misran, Novel high performance hollow fiber ultrafiltration membranes spun from LiBr doped solutions, Desalination 249 (2009) 541–548.
[22] M.Z. Yunos, Z. Harun, H. Basri, A.F. Ismail, Effects of water as non-solvent additive on performance of polysulfone ultrafiltration membrane, Adv. Mater. Res. 488–489 (2012) 46–50.
[23] A. Xu, A. Yang, S. Young, D. deMontigny, P. Tontiwachwuthikul, Effect of internal coagulant on effectiveness of polyvinylidene fluoride membrane for carbon dioxide separation and absorption, J. Membr. Sci. 311 (2008) 153–158.
[24] H. Basri, A.F. Ismail, M. Aziz, Polyethersulfone (PES)–silver composite UF membrane: effect of silver loading and PVP molecular weight on membrane morphology and antibacterial activity, Desalination 273 (2011) 72–80.
[25] Y. Zhang, Z. Jin, X. Shan, J. Sunarso, P. Cui, Preparation and characterization of phosphorylated Zr-doped hybrid silica/PSF composite membrane, J. Hazard. Mater. 186 (2011) 390–395.
[26] S. Wongchitphimon, R. Wang, R. Jiraratananon, L. Shi, C.H. Loh, Effect of polyethylene glycol (PEG) as an additive on the fabrication of polyvinylidene fluoride-co-hexafluropropylene (PVDF–HFP) asymmetric microporous hollow fiber membranes, J. Membr. Sci. 369 (2011) 329–338.
[27] Y. Ma, F. Shi, J. Ma, M. Wu, J. Zhang, C. Gao, Effect of PEG additive on the morphology and performance of polysulfone ultrafiltration membranes, Desalination 272 (2011) 51–58.
[28] J.-H. Kim, K.-H. Lee, Effect of PEG additive on membrane formation by phase inversion, J. Membr. Sci. 138 (1998) 153–163.
[29] B. Chakrabarty, A.K. Ghoshal, M.K. Purkait, Effect of molecular weight of PEG on membrane morphology and transport properties, J. Membr. Sci. 309 (2008) 209–221.
[30] D.Y. Koseoglu-Imer, B. Kose, M. Altinbas, I. Koyuncu, The production of polysulfone (PS) membrane with silver nanoparticles (AgNP): physical properties, filtration performances, and biofouling resistances of membranes, J. Membr. Sci. 428 (2013) 620–628.
[31] F.-Q. Nie, Z.-K. Xu, P. Ye, J. Wu, P. Seta, Acrylonitrile-based copolymer membranes containing reactive groups: effects of surface-immobilized poly(ethylene glycol)s on anti-fouling properties and blood compatibility, Polymer 45 (2004) 399–407.
[32] L.-P. Zhu, L. Xu, B.-K. Zhu, Y.-X. Feng, Y.-Y. Xu, Preparation and characterization of improved fouling-resistant PPESK ultrafiltration membranes with amphiphilic PPESK-graft-PEG copolymers as additives, J. Membr. Sci. 294 (2007) 196–206.
[33] D.H. Kim, S.-H. Moon, J. Cho, Investigation of the adsorption and transport of natural organic matter (NOM) in ion-exchange membranes, Desalination 151 (2003) 11–20.
[34] B.D. McCloskey, H.B. Park, H. Ju, B.W. Rowe, D.J. Miller, B.J. Chun, K. Kin, B.D. Freeman, Influence of polydopamine deposition conditions on pure water flux and foulant adhesion resistance of reverse osmosis, ultrafiltration, and microfiltration membranes, Polymer 51 (2010) 3472–3485.
[35] J. Labanowski, G. Feuillade, Dissolved organic matter: precautions for the study of hydrophilic substances using XAD resins, Water Res. 45 (2011) 315–327.
[36] H. Hua, N. Li, L. Wu, H. Zhong, G. Wu, Z. Yuan, X. Lin, L. Tang, Anti-fouling ultrafiltration membrane prepared from polysulfone-graft-methyl acrylate copolymers by UV-induced grafting method, J. Environ. Sci. 20 (2008) 565–570.
[37] Q.-Z. Zheng, P. Wang, Y.-N. Yang, Rheological and thermodynamic variation in polysulfone solution by PEG introduction and its effect on kinetics of membrane formation via phase-inversion process, J. Membr. Sci. 279 (2006) 230–237.
[38] G.R. Guillen, Y. Pan, M. Li, E.M.V. Hoek, Preparation and characterization of membranes formed by nonsolvent induced phase separation: a review, Ind. Eng. Chem. Res. 50 (2011) 3798–3817.
[39] J.-f. Li, Z.-l. Xu, H. Yang, C.-p. Feng, J.-h. Shi, Hydrophilic Microporous PES Membranes Prepared by PES/PEG/DMAc Casting Solutions, 2007.
[40] A.W. Zularisam, A.F. Ismail, R. Salim, Behaviours of natural organic matter in membrane filtration for surface water treatment — a review, Desalination 194 (2006) 211–231.
[41] A.W. Zularisam, A.F. Ismail, M.R. Salim, M. Sakinah, H. Ozaki, The effects of natural organic matter (NOM) fractions on fouling characteristics and flux recovery of ultrafiltration membranes, Desalination 212 (2007) 191–208.